Nuclear Imaging of Met-Expressing Human and Canine Cancer Xenografts with Radiolabeled Monoclonal Antibodies (MetSeek™)

Rick V. Hay,[1] Brian Cao,[1] R. Scot Skinner,[2] Yanli Su,[1] Ping Zhao,[1] Margaret F. Gustafson,[1] Chao-Nan Qian,[1] Bin T. Teh,[1] Beatrice S. Knudsen,[3] James H. Resau,[1] Shuren Shen,[4] David J. Waters,[4] Milton D. Gross,[2] and George F. Vande Woude[1]

Abstract

Purpose: Met, an oncogene product and receptor tyrosine kinase, is a keystone molecule for malignant progression in solid human tumors. We are developing Met-directed imaging and therapeutic agents, including anti-Met monoclonal antibodies (MetSeek™). In this study, we compared two antibodies, Met5 and Met3, for nuclear imaging of human and canine Met-expressing tumor xenografts in nude mice.

Experimental Design: Xenografts representing cancers of three different human tissue origins and metastatic canine prostate cancer were raised s.c. in host athymic nude mice. Animals were injected i.v. with I-125-Met5 or I-125-Met3, posterior total body gamma camera images were acquired for several days postinjection, and quantitative region-of-interest activity analysis was done.

Results: PC-3, SK-LMS-1/HGF, and CNE-2 xenografts imaged with I-125-Met5 were compared with PC-3, SK-LMS-1/HGF, and DU145 xenografts imaged with I-125-Met3. Nuclear imaging contrast was qualitatively similar for I-125-Met5 and I-125-Met3 in PC-3 and SK-LMS-1/HGF host mice. However, by region-of-interest analysis, the set of human tumors imaged with I-125-Met3 exhibited a pattern of rapid initial tumor uptake followed by a continuous decline in activity, whereas the set of human tumors imaged with I-125-Met5 showed slow initial uptake, peak tumor-associated activity at 1 day postinjection, and persistence of activity in xenografts for at least 5 days. GN4 canine prostate cancer xenografts were readily imaged with I-125-Met5.

Conclusions: We conclude that radioiodinated Met3 and Met5 offer qualitatively similar nuclear images in xenograft-bearing mice, but quantitative considerations indicate that Met5 might be more useful for radioimmunotherapy. Moreover, canine prostate cancer seems to be a suitable model for second-stage preclinical evaluation of Met5.

Met, a receptor tyrosine kinase and oncogene product, is a keystone molecule for the initiation and malignant progression of solid neoplasms in humans and in experimental animal models of cancer (1). The myriad sequelae of Met activation, either following interaction with its native ligand hepatocyte growth factor/scatter factor (HGF/SF), with surrogate ligands (2, 3), or through ligand-independent pathways, include cell proliferation, migration, differentiation, and survival. In normal cells, these events are responsible for such phenomena as the epithelial-to-mesenchymal transformation responsible for limb muscle and diaphragm formation, and the formation of ductular glands. In neoplastic cells, these events are recapitulated as tumor formation, invasion, metastasis, and the prevention of apoptosis. Indeed, the plasticity involved in the initial seeding and subsequent growth of tumor metastases—which requires switching cells from an invasive to a proliferative state—can be accounted for in some experimental systems by ligand-dependent activation of Met (4).

Virtually any type of solid tumor can express Met and/or its ligand abnormally (by overabundance, mutation, or dysregulation; see online Table 1 in ref. 1), http://www.vai.org/vari/metandcancer/index.aspx). The prevalence of abnormal Met expression is typically higher in metastases than in primary lesions, and is associated with poor clinical prognosis. In fact, some highly aggressive human cancers (glioblastoma multiforme, osteosarcoma, and osseous metastases of prostate cancer) reportedly *always* exhibit abnormal Met expression. We have proposed that Met should be exploited as a clinical marker for distinguishing those cancers most likely to behave aggressively from less-threatening ones (5).

Authors' Affiliations: [1]Van Andel Research Institute, Grand Rapids, Michigan; [2]Department of Veterans Affairs Healthcare System, Ann Arbor, Michigan; [3]Fred Hutchinson Cancer Research Center, Seattle, Washington; and [4]Gerald P. Murphy Cancer Foundation, West Lafayette, Indiana

Grant support: Michigan Life Sciences Corridor (to M.D. Gross and G.F. Vande Woude), Cap CURE (to B.S. Knudsen), the Michigan Universities Commercialization Initiative (to R.V. Hay), the Jay and Betty Van Andel Foundation (to B. Cao, B.T. Teh, J.H. Resau, and G.F. Vande Woude), and the Department of Veterans Affairs (to M.D. Gross).

Presented at the Tenth Conference on Cancer Therapy with Antibodies and Immunoconjugates, October 21-23, 2004, Princeton, New Jersey.

Requests for reprints: Rick V. Hay, Van Andel Research Institute, 333 Bostwick NE, Grand Rapids, MI 49503. Phone: 616-234-5726; Fax: 616-234-5727; E-mail: Rick.Hay@vai.org.

doi:10.1158/1078-0432.CCR-1004-0014

Our laboratories are collaboratively developing Met-directed agents for diagnostic and therapeutic applications, including monoclonal antibodies (mAb) that interfere with the binding of HGF/SF to Met (6), geldanamycins (7), RNA interference (8), and mAbs that recognize the extracellular domain of Met (8). We have been evaluating the last category, designated "MetSeek™", for its potential usefulness in radioimmunoscintigraphy and possibly radioimmunotherapy (9–12). Our previous reports have shown that Met3 (also known as 2F6, a mAb that recognizes a human-specific epitope of Met), either alone or in combination with a neutralizing mixture of anti-HGF/SF mAbs, can be radiolabeled and used to image a variety of autocrine and paracrine Met-expressing human tumor xenografts in nude mice with high specificity and with a signal proportional to Met abundance in the respective parental cell lines (9, 10).

In this article, we summarize our experience performing preclinical radioimmunoscintigraphy with Met5 (a mAb that recognizes an epitope common to the extracellular domains of human and canine Met), comment on potential advantages of Met5 over Met3, and propose further preclinical evaluation of Met5.

Materials and Methods

Reagents. I-125 was purchased as NaI [480-630 MBq (13-17 mCi)/μg iodine] from Amersham Corp. (Arlington Heights, IL). All other reagents were of the best commercial grade available.

Cell lines and tumor induction. All parental cell lines used for xenograft induction were maintained in DMEM containing 10% fetal bovine serum. Data are presented here for xenografts derived from the stable lines SK-LMS-1/HGF (human leiomyosarcoma cell line autocrine for human Met and human HGF/SF; refs. 10, 13), PC-3 and DU145 (paracrine Met-expressing human prostate carcinoma cell lines; refs. 8, 10, 14), CNE-2 (poorly differentiated paracrine Met-expressing human nasopharyngeal carcinoma cell line; ref. 15), and GN4 (Met-expressing canine prostate cancer cell line established from pulmonary metastasis; ref. 16).

Female athymic nude (*nu/nu*) mice at about 6 weeks of age received s.c. injections of parental cell line suspensions in the posterior aspect of their right thighs. Each mouse received between 2×10^5 and 5×10^5 cells. Tumors developed for 2 to 6 weeks, reaching >0.5 cm in greatest dimension by external caliper measurement before imaging. Mice were housed in small groups and given *ad libitum* access to mouse chow and drinking water under conditions approved by the institutional animal care committees.

Preparation and characterization of monoclonal antibodies. A panel of full-length murine mAbs against the extracellular domain of human Met was produced and screened for reactivity as previously described (9). Antibodies from clone 2F6 were subsequently designated "Met3" (10). The mAb Met5 was produced and screened concurrently with Met3. Met3 recognizes an epitope present on human but not canine Met, whereas Met5 recognizes an epitope common to the extracellular domains of human and canine Met. The irrelevant, negative-control mAb LF7 was raised against the purified lethal factor subunit of *Bacillus anthracis* lethal toxin. Met3 is of antibody type IgG_{2b}, Met5 of type IgG_1, and LF7 of type IgG_1.

For nuclear imaging experiments, IgG fractions were purified from Met5, Met3, and LF7 hybridoma cell line supernatant fractions by protein G affinity chromatography and adjusted to a final concentration of 2 mg/mL in 0.25 mol/L sodium phosphate buffer (pH 6.8-7.0). The purified IgG fractions were stored frozen in small aliquots (25-50 μg) and thawed just prior to radioiodination.

Radioiodination and injection of monoclonal antibodies. Met5, Met3, and LF7 were radioiodinated by the procedure described previously (9). Briefly, to 25 μg of mAb in 0.1 mL of 0.25 mol/L sodium phosphate (pH 6.8) was added 74 MBq (2.0 mCi; 0.02 mL) of I-125 as sodium iodide and 20 nmol (0.01 mL) of chloramine T. The reactants were mixed and agitated gently for 90 seconds at room temperature. The reaction was quenched by the addition of 42 nmol (0.02 mL) of sodium metabisulfite. I-125-mAb was separated from nonreacted I-125 by ion exchange on a small column of Bio-Rad (Hercules, CA) AG 1 X8 resin (50-100 mesh).

Radiolabeling efficiency was determined in a Beckman Gamma 8000 counter, and the proportion of protein-bound I-125 in the final product was assessed by chromatography on ITLC-SG strips (Pall Corp., East Hills, NY) developed in 80% aqueous methanol. Assuming complete recovery of mAb from the labeling mixture, radiolabeling efficiency was >60%, and protein-bound radioactivity accounted for >90% of total activity in the final product.

To minimize loss of immunoreactivity or binding affinity resulting from radioiodination, we employ chloramine T reaction conditions that bind only one atom of radioiodine per molecule of protein; store radioiodinated protein at 4°C until use; and inject radiolabeled proteins into animals within 24 hours of labeling. Although we have no direct *in vitro* measurements of immunoreactivity or binding affinity of I-125-MetSeek, preliminary studies using a novel radiometal-labeled Met3 immunoconjugate that exhibits preserved immunoreactivity *in vitro* yield scintigrams comparable to those generated with I-125-Met3,[5] indicating that the method of radioiodination used here does not significantly alter the binding characteristics of MetSeek mAbs.

Imaging procedures and analysis. Animals were imaged and scintigrams were analyzed by previously established methods (9, 10, 17, 18). In brief, each mouse received I-125-labeled Met5, Met3, or LF7, 50 to 100 μCi (1.8-3.7 MBq), representing 1.2 to 2.5 μg of protein, in ~50 μL i.v. by tail vein injection under light inhalation anesthesia. Just prior to each imaging session, each mouse was given up to 13 mg/kg xylazine and 87 mg/kg ketamine s.c. in the interscapular region.

Posterior whole-body gamma camera images of each mouse were acquired beginning at 1 to 2 hours following I-125-labeled mAb injection and again at 1, 3, and 5 to 7 days postinjection. Sedated mice were placed singly or in pairs on top of an inverted camera head with a protective layer over the collimator, and taped to the layer to maintain optimum limb extension. Images of I-125 activity were acquired on a Siemens LEM Plus mobile camera with a low-energy, high-sensitivity collimator. Acquisitions were obtained over a period of 15 minutes, during which we collected between 2×10^5 and 3×10^6 counts per total body image.

Relative activity was determined by computer-assisted region-of-interest analysis for each tumor, for total body, and for appropriate background regions at each imaging time point. Regional counts are converted to activity (in microcuries) by interpolation, using a standard curve generated by imaging diluted samples of known activity under similar geometry for the particular camera, radionuclide, and acquisition settings employed for the animal imaging protocol. In order to compensate for the potentially high variability (±10%) in the small injectate volumes used for these experiments, we assume that the total body activity measured for an individual host mouse at the earliest imaging time point (1-2 hours postinjection, when total body clearance of full-length mAbs is still negligible) more closely approximates the actual injected activity received by that mouse than does the "nominal injected activity" attributed to a presumed injectate volume. We designate this variable "estimated injected activity," and therefore set total body activity at the earliest imaging time point = 100% estimated injected activity. All region-of-interest counting values for tumor-associated radioactivity are corrected for background and physical

[5] Hay R.V., unpublished data.

decay, normalized to this variable for each individual host mouse, and expressed as "the percentage of estimated injected activity." Graphical and statistical analysis of the converted data used the program Excel (Microsoft).

Results

Figure 1 shows serial total body gamma camera images of individual mice bearing Met-expressing human cancer xenografts from diverse tissue origins, between 1 hour and 5 days following i.v. injection of I-125-Met5. Asymmetrical distribution of hind limb activity is suggested in the PC-3 and CNE-2 xenograft hosts at the earliest imaging session, with focal accumulation evident at 1 hour postinjection only in the SK-LMS-1/HGF host. Tumor-associated radioactivity as a function of total body activity is prominent in all three xenograft hosts by 1 day postinjection, and activity in the tumors persists through the final imaging session. In qualitative terms, these scintigrams are comparable to those we previously obtained with I-125-Met3 (see Fig. 3 of ref. 10), and superimposable plots of "image contrast" (expressed as tumor/total body activity ratios over time) for I-125-Met3 and I-125-Met5 were obtained for both SK-LMS-1/HGF hosts (highest ratio 0.146 ± 0.097 for Met5 versus 0.168 ± 0.076 for Met3; see Fig. 5 of ref. 10) and PC-3 hosts (highest ratio 0.086 ± 0.043 for Met5 versus 0.101 ± 0.045 for Met3).

Figure 2 shows graphical results of quantitative image region-of-interest analysis, expressed as the percentage of estimated injected activity associated with xenografts of differing tissue origin as a function of time postinjection. As we previously reported (10), each xenograft host group injected with I-125-Met3 (open symbols) exhibited the highest mean value for this function at the earliest imaging session, with respective values of 7.2 ± 2.2%, and 5.4 ± 2.6% of the estimated injected activity for SK-LMS-1/HGF and PC-3 (these two plots are reproduced from ref. 9), and declined continuously thereafter. The time-activity plots for xenograft-associated activity in DU145 hosts and PC-3 hosts injected with I-125-Met3 were superimposable.

In comparison, by region-of-interest analysis, each host group injected with I-125-Met5 (Fig. 2, solid symbols) exhibited the highest mean value for percentage of estimated injected activity associated with xenografts at 1 day postinjection, with respective values of 7.5 ± 3.4%, 13.3 ± 7.6%, and 12.3 ± 4.3% of the estimated injected activity for PC-3, SK-LMS-1/HGF, and CNE-2, and with activity persisting in the xenografts at 6% to 10% of estimated injected activity through the final imaging session.

For hosts injected with the irrelevant antibody I-125-LF7 (plotted with asterisks), mean activity in SK-LMS-1/HGF xenografts accounted for <3% of estimated injected activity and <4% of total body activity at any time postinjection.

In order to reinforce our empirical basis for conducting second-stage preclinical evaluation of new Met-directed diagnostic and therapeutic agents in dogs with spontaneous cancers (see Discussion), we have used Met5 to image mice bearing tumor xenografts derived from previously established canine prostate cancer cell lines (16). Figure 3 displays serial I-125-Met5

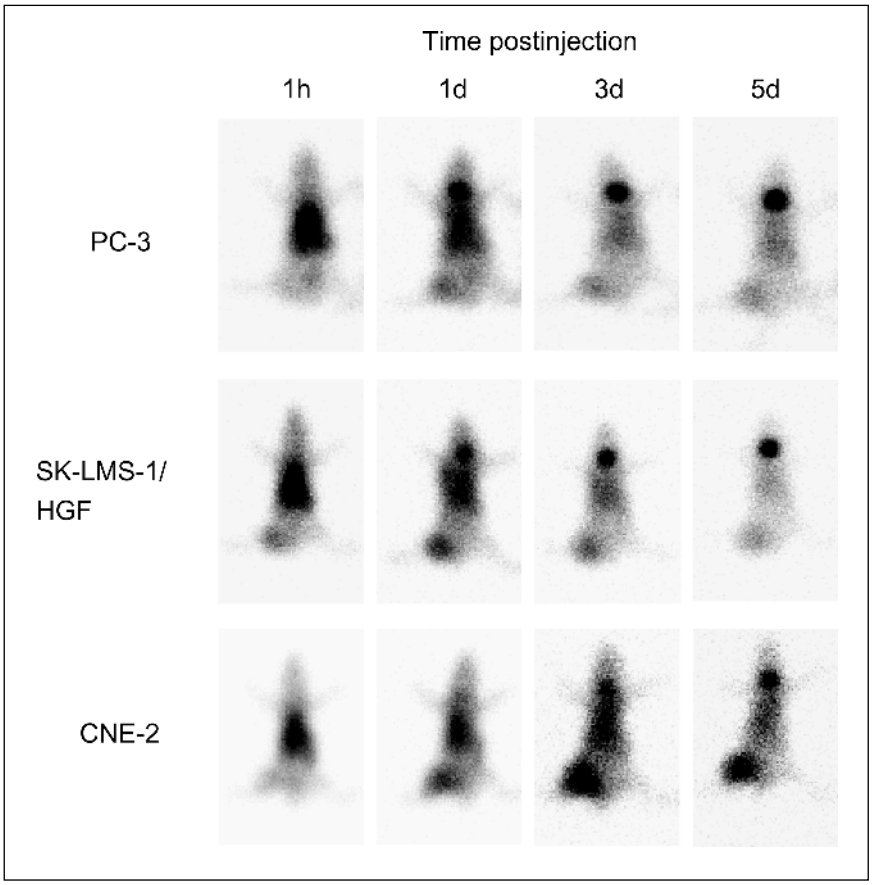

Fig. 1. Met5 scintigrams of mice bearing human tumor xenografts. The indicated Met-expressing human cancer cell lines were injected s.c. in the posterior aspect of the right thighs of female athymic nude mice to induce xenografts. Host animals underwent radioimmunoscintigraphy with I-125-Met5 (50-100 μCi given i.v.) when their tumors reached >0.5 cm in greatest dimension. A composite of serial posterior whole body scintigrams for individual animals bearing tumors as indicated on the left is shown, from 1 hour to 5 days postinjection. The craniadmost focus of activity in 1- to 5-day postinjection images represents liberated radioiodide uptake by the thyroid.

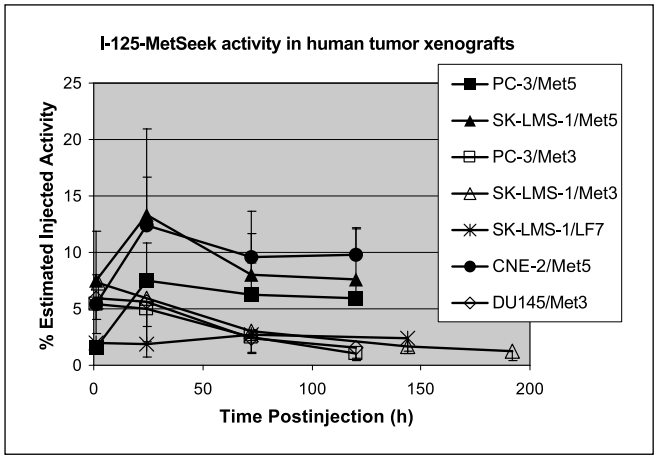

Fig. 2. Region-of-interest analysis of Met5 and Met3 scintigrams. Serial scintigrams for each host animal were evaluated by quantitative region-of-interest analysis. The graph depicts the percentage of estimated injected activity associated with the tumor xenografts as a function of time postinjection. Mean values (± 1 SD) are shown at each time point postinjection for each xenograft host group (n = 3-5 animals/group). Solid symbols, host groups injected with I-125-Met5; open symbols, host groups injected with I-125-Met3; asterisks, SK-LMS-1/HGF host group injected with the irrelevant antibody I-125-LF7. The plots for PC-3 and SK-LMS-1/HGF host groups injected with I-125-Met3 are reproduced from Hay et al. (9).

scintigrams obtained from a single mouse bearing a GN4 xenograft, which exhibit a qualitative pattern similar to that seen with the CNE-2 host in Fig. 1.

Figure 4 displays the results of region-of-interest analysis of scintigrams obtained from GN4 host mice injected with either I-125-Met5 (which recognizes an epitope common to human and canine Met) or I-125-Met3 (which recognizes human but not canine Met). Just as we observed with Met-expressing human tumor xenografts imaged with Met5 (Fig. 2), the GN4 host group injected with I-125-Met5 exhibited the highest mean value for percentage of estimated injected activity associated with tumors at 1 day postinjection, reaching 16.8 ± 4.8% of the estimated injected activity. By visual analysis, image contrast increased during the experiment; and by region-of-interest analysis, GN4-associated radioactivity following injection of host mice with I-125-Met5 accounted for mean values of 19.6%, 22.1%, and 24.2% of total body activity, respectively, at 1, 3, and 5 days postinjection. Preliminary results suggest that xenografts derived from TR6LM canine prostate cancer cells (16), which are very sensitive to small-interfering RNA constructs that target Met (8), exhibit a similar pattern and magnitude of I-125-Met5 uptake and retention (data not shown).

Animals injected with I-125-Met3 as a negative control agent showed a value of 11.0 ± 8.6% estimated injected activity in tumors at 1 day postinjection; however, we consider this an unreliable measurement, given its disproportionately high SD compared with the other data points. Calculated Met5/Met3 activity ratios in GN4 tumors were 2.8 and 2.9, respectively, at 3 and 5 days postinjection.

Discussion

With this and our previous reports (9, 10), we have established that two full-length murine anti-Met mAbs (MetSeek™), designated Met5 and Met3, are useful for preclinical radioimmunoscintigraphy of human tumor xenografts. Radioiodinated Met5 and Met3 generate qualitatively comparable nuclear images in this mouse model, with nearly identical peak image contrast observed in two tumor types (cf. Fig. 1 of this article and of ref. 9). However, by quantitative region-of-interest analysis, the time-activity curves of tumor activity exhibit two distinct patterns (Fig. 2). A "Met3" pattern is characterized by rapid initial tumor uptake of radiolabeled anti-Met mAb and followed by continuous decline of activity, so that the greatest fraction of injected activity is found in the tumors at the earliest imaging time point, typically 1 to 2 hours postinjection. A "Met5" pattern, in contrast, is characterized by slow initial tumor uptake of anti-Met mAb, peaking at 1 day postinjection and followed by the persistence of tumor-associated radioactivity for several days.

How these detailed quantitative differences are manifested at the molecular level (e.g., Met receptor turnover, surface availability) is not known. Regardless of its molecular basis, the difference between Met3 and Met5 patterns of mAb uptake and retention *in vivo* carries potentially important clinical implications: Because radiation exposure of a tumor is related to the integral of the time-activity curve, as a first approximation Met5 would seem to be more effective than Met3 for radioimmunotherapy, whereas Met3 might permit a more rapid diagnostic imaging protocol with lower patient exposure risk.

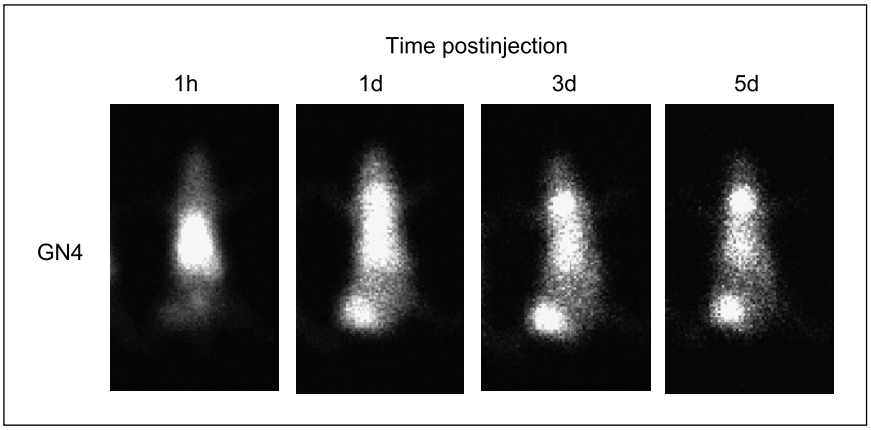

Fig. 3. Serial Met5 scintigrams of a mouse bearing a GN4 canine prostate cancer xenograft. GN4 cells were injected s.c. in the posterior aspect of the right thighs of five female athymic nude mice to induce tumor xenografts. Host animals underwent radioimmunoscintigraphy with I-125-Met5 (78 μCi given i.v.) when their tumors reached ›0.5 cm in greatest dimension. Serial posterior whole body scintigrams for a single host animal are shown, from 1 hour to 5 days postinjection.

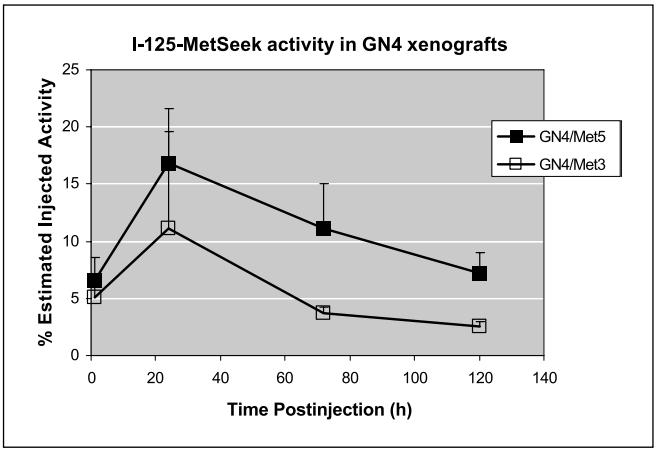

Fig. 4. Region-of-interest analysis of Met5 and Met3 scintigrams from GN4 xenograft-bearing mice. Mice bearing GN4 xenografts were injected with I-125-Met5 as described in the legend to Fig. 3, and an additional five mice bearing GN4 xenografts were injected with I-125-Met3 (109 μCi given i.v.). Serial scintigrams for each host animal were evaluated by quantitative region-of-interest analysis. The graph depicts the percentage of estimated injected activity associated with the tumor xenografts as a function of time postinjection. Mean values (± 1 SD) are shown at each time point postinjection for each xenograft host group (n = 5 animals/group).

Although our findings constitute satisfactory proof-of-principle for the use of MetSeek™ in nuclear imaging studies, the heterotopic xenograft-bearing mouse model we have used here poses particular barriers to a more sophisticated evaluation of new Met-directed diagnostic and therapeutic agents. First, paracrine Met-expressing human tumor xenografts, such as PC-3 and DU145, do not flourish in standard strains of nude or severe combined immunodeficiency mice, because murine HGF/SF does not interact appreciably with human Met. However, with our laboratories' recent development of an immunocompromised mouse strain transgenic for human HGF/SF (19), and improved techniques for generating orthotopic and metastatic xenografts (20), we expect that more robust tumor growth and easier generation of metastatic lesions will follow.

Secondly, the development of new murine systems notwithstanding, none of our MetSeek™ reagents recognizes the murine Met expressed by normal tissues. Thus, we cannot conduct a meaningful biodistribution analysis of radiolabeled anti-Met mAbs in mice as the next logical step in seeking regulatory approval for human clinical use.

We have therefore turned to canine cancer as a valuable second-stage preclinical model for agent evaluation. Canine prostate cancer has many similarities to human prostate cancer, including the development of high-grade intraepithelial neoplasia (21) and progression to invasive prostate carcinoma (22). One of our laboratories has conducted an extensive analysis of the clinical and pathologic features of canine prostate carcinoma (23), as well as a detailed study of pet dogs in which spontaneous cancers first presented as bony metastases (24), and collaboratively established stable cultured canine prostate carcinoma cell lines (16). We have recently shown that some of these lines overexpress Met, and that at least one is sensitive to small-interfering RNA constructs that target Met (8).

With our additional demonstration in this report that xenografts induced by GN4 (a canine prostate cancer cell line derived from a pulmonary metastasis) can be imaged with radiolabeled Met5 in a fashion similar to human cancer xenografts in the same model—and with better imaging signals than the Met-expressing human prostate cancer xenografts—we now have a solid empirical basis for proceeding to Met-directed imaging, biodistribution, and therapeutic studies in living dogs with cancer. We note that an exciting precedent for this approach has been established by Anidjar et al. (25), who used an I-131-labeled mAb reactive with human prostate-specific membrane antigen to image a canine prostate cancer allograft in an immunodeficient dog.

Finally, because both Met3 and Met5 activate Met in tumor cell lines *in vitro*, and because Met activation by naturally occurring ligand can result in dramatic changes in Met expression and in cell surface exposure, it would be difficult to use radioimmunoscintigraphy with full-length mAbs to obtain better than a relative approximation of Met abundance *in vivo*, as we have previously described for Met3 (10). Therefore, we have recently begun evaluating monovalent anti-Met constructs that neither activate nor inhibit Met as alternate quantitative imaging probes, including a new human anti-Met Fab described elsewhere (26).

Acknowledgments

We thank Troy Carrigan for expert administrative assistance. This manuscript is dedicated to the memory of Jay and Betty Van Andel.

References

1. Birchmeier C, Birchmeier W, Gherardi E, Vande Woude GF. Met, metastasis, motility and more. Nat Rev Mol Cell Biol 2003;4:915–25.
2. Banerjee M, Copp J, Vuga D, et al. GW domains of the *Listeria monocytogenes* invasion protein InlB are required for potentiation of Met activation. Mol Microbiol 2004;52:257–71.
3. Carrolo M, Giordano S, Cabrita-Santos L, et al. Hepatocyte growth factor and its receptor are required for malaria infection. Nat Med 2003;9:1363–9.
4. Gao C-F, Xie Q, Su Y-L, et al. Proliferation and invasion: Plasticity in tumor cells. Proc Natl Acad Sci U S A 2005;102:10528–33.
5. Hay R, Cao B, Tsarfaty I, Tsarfaty G, Resau J, Vande Woude G. Grappling with metastatic risk: bringing molecular imaging of Met expression toward clinical use. J Cell Biochem 2002;Suppl 39:184–93.
6. Cao B, Su Y, Oskarsson M, et al. Neutralizing monoclonal antibodies to hepatocyte growth factor/scatter factor (HGF/SF) display antitumor activity in animal models. Proc Natl Acad Sci U S A 2001;98:7443–8.
7. Webb CP, Hose CD, Koochekpour S, et al. The geldanamycins are potent inhibitors of the HGF/SF-Met-uPA-plasmin proteolytic network. Cancer Res 2000; 60:342–9.
8. Shinomiya N, Gao CF, Xie Q, et al. RNA interference reveals that ligand-independent met activity is required for tumor cell signaling and survival. Cancer Res 2004;64:7962–70.
9. Hay RV, Cao B, Skinner RS, et al. Radioimmunoscintigraphy of tumors autocrine for human Met and hepatocyte growth factor/scatter factor. Mol Imaging 2002;1:56–62.
10. Hay RV, Cao B, Skinner RS, et al. Radioimmunoscintigraphy of human Met-expressing tumor xenografts using Met3, a new monoclonal antibody. Clin Cancer Res 2003;9:3839–44s.
11. Hay RV, Cao B, Skinner RS, et al. Met5, a new monoclonal antibody for radioimmunoscintigraphy of Met-expressing tumors [abstract]. J Nucl Med 2003; 44:178P.
12. Hay R, Cao B, Skinner S, et al. Uptake of radiolabeled anti-Met monoclonal antibodies by canine and human prostate cancer xenografts [abstract]. Cancer Biother Radiopharm 2004;19:521.
13. Jeffers M, Rong S, Vande Woude GF. Enhanced tumorigenicity and invasion-metastasis by hepatocyte growth factor/scatter factor-met signaling in human cells concomitant with induction of the urokinase proteolysis network. Mol Cell Biol 1996;16:1115–25.
14. Knudsen BS, Gmyrek GA, Inra J, et al. High expression of the Met receptor in prostate cancer metastasis to bone. Urology 2002;60:1113–7.

15. Qian C-N, Guo X, Cao B, et al. Met protein expression level correlates with survival in patients with late-stage nasopharyngeal carcinoma. Cancer Res 2002; 62:589–96.

16. Walker-Daniels J, Coffman K, Azimi M, et al. Overexpression of the EphA2 tyrosine kinase in prostate cancer. Prostate 1999;41:275–80.

17. Gross MD, Skinner RWS, Grossman HB. Radioimmunodetection of a transplantable human bladder carcinoma in a nude mouse. Invest Radiol 1984;19: 530–4.

18. Hay RV, Skinner RS, Newman OC, et al. Scintigraphy of acute inflammatory lesions in rats with radiolabelled recombinant human interleukin-8. Nucl Med Commun 1997;18:367–78.

19. Zhang YW, Su Y, Lanning N, et al. Enhanced growth of human met-expressing xenografts in a new strain of immunocompromised mice transgenic for human hepatocyte growth factor/scatter factor. Oncogene 2005;24:101–6.

20. Qian C-N, Takahashi M, Kahnoski RJ, Teh BT. 2003. Effect of sildenafil citrate on an orthotopic prostate cancer growth and metastasis model. J Urol 2003; 170:994–7.

21. Waters DJ. High-grade prostatic intraepithelial neoplasia in dogs. Eur Urol 1999;35:456–8.

22. Aquilina JW, McKinney L, Pacelli A, et al. High grade prostatic intraepithelial neoplasia in military working dogs with and without prostate cancer. Prostate 1998;36:189–93.

23. Cornell KK, Bostwick DG, Cooley DM, et al. Clinical and pathologic aspects of spontaneous canine prostate carcinoma: a retrospective analysis of 76 cases. Prostate 2000;45:173–83.

24. Cooley DM, Waters DJ. Skeletal metastases as the initial clinical manifestation of metastatic carcinoma in 19 dogs. J Vet Intern Med 1998;12:288–93.

25. Anidjar M, Villette JM, Devauchelle P, et al. *In vivo* model mimicking natural history of dog prostate cancer using DPC-1, a new canine prostate carcinoma cell line. Prostate 2001;46:2–10.

26. Jiao Y, Zhao P, Zhu J, et al. Construction of human naïve Fab library and characterization of anti-Met Fab fragment generated from the library. Mol Biotech. In press 2005.

Clinical Cancer Research

Nuclear Imaging of Met-Expressing Human and Canine Cancer Xenografts with Radiolabeled Monoclonal Antibodies (MetSeek ™)

Rick V. Hay, Brian Cao, R. Scot Skinner, et al.

Clin Cancer Res 2005;11:7064s-7069s.